

Rendezvous Design in a Cislunar Near Rectilinear Halo Orbit

Emmanuel Blazquez¹, Laurent Beauregard¹, Stéphanie Lizy-Destrez¹, Finn Ankensen² and Francesco Capolupo³

¹ Institut Supérieur de l'Aéronautique et de l'Espace (ISAE-SUPAERO), 10 Avenue Edouard Belin, 31400 Toulouse, France

² European Space Agency, Keplerlaan 1, 2201 AZ Noordwijk, The Netherlands

³ Airbus Defence and Space, 31 rue des Cosmonautes, 31400 Toulouse, France

Abstract

In the context of future Human Spaceflight exploration missions, Rendezvous and Docking (RVD) activities are critical for the assembly and maintenance of cislunar structures. The scope of this research is to investigate the specifics of orbits of interest for RVD in the cislunar realm and to propose novel strategies to safely perform these kinds of operations. This paper focuses on far rendezvous approaches and passively safe drift trajectories in the ephemeris model. The goal is to exhibit phasing orbit requirements to ensure safe far approach. Ephemeris representations of Near Rectilinear Halo Orbits (NRHOs) were derived using multiple shooting and adaptive receding-horizon targeting algorithms. Simulations showed significant drift and overlapping properties for phasing and target orbits of interest, motivating the search for safe natural drift trajectories, using impact prediction strategies.

Keywords: Rendezvous, Near Rectilinear Halo Orbits, Ephemeris, Trajectory design, Safety.

Introduction

The future Lunar Orbital Platform Gateway will require cargo delivery and crew exchange operational activities, both which rely critically on Rendezvous and Docking operations (RVD) with modules such as Orion [1]. The RVD problem in Keplerian dynamics has been extensively discussed. However, to this date, no operational RVD has yet been performed in the vicinity of a Lagrangian point. Missions involving the Gateway and the Orion spacecraft have kick-started a new trend of publications and research on proximity operations in the cislunar realm. Near Rectilinear Halo Orbits (NRHOs) have been identified as suitable orbits to host the Gateway and to accommodate multiple mission staging [2].

The scope of this research is to propose novel methodologies and trajectory designs to accommodate the constraints of rendezvous operations between a “chaser” spacecraft and a “target” orbiting platform in a non-Keplerian environment. Previous contributions from the authors have investigated traditional far-approach strategies, as well as close rendezvous dynamics using linear and non-linear targeting algorithms [3]. This paper proposes a new strategy for far rendezvous operations in non-Keplerian environments, exploiting safe free-drift in the ephemeris model. Such trajectories result in significantly low ΔV budgets to safely reach the vicinity of the target, from where to engage in close proximity operations.

Near Rectilinear Halo Orbits in High-fidelity Models

The Circular Restricted Three-Body Problem (CR3BP)

The CR3BP describes the motion of a massless body P under the gravitational influence of two massive primaries orbiting circularly about one another, with masses m_1 and m_2 respectively and $m_1 > m_2$. The mass parameter $\mu = \frac{m_2}{m_1 + m_2}$ is introduced. The motion is studied in a barycentric, adimensional, rotating reference frame called the synodic frame, so

that the primaries rotate counterclockwise about their barycentre and are fixed on the x axis at $(-\mu, 0, 0)$ and $(1-\mu, 0, 0)$ respectively.

The differential equations describing the motion of the massless particle P are: [4]

$$\begin{cases} \ddot{x} - 2\dot{y} = -U_x \\ \ddot{y} + 2\dot{x} = -U_y \\ \ddot{z} = -U_z \end{cases} \quad (1)$$

Where U_x , U_y and U_z are the Cartesian partial derivatives of the gravitational potential U .

The Ephemeris Model

The Ephemeris model describes the motion of a massless body P under the gravitational field generated by $N-1$ massive primaries. The absolute state of the primaries is given by ephemeris of the precise positions and velocities of the bodies over time in the Earth-centered inertial frame J2000. Each primary is described by its standard gravitational parameter μ_i and its absolute position vector \mathbf{X}_i .

The second-order differential equation describing the evolution of the position vector $\mathbf{X}(t)$ of the massless particle P , relative to the position of the first primary in the J2000 frame is: [5]

$$\ddot{\mathbf{X}} = -\mu_1 \frac{\mathbf{X}}{\|\mathbf{X}\|^3} - \sum_{i=2}^{N-1} \mu_i \left(\frac{\mathbf{X} - \mathbf{X}_i}{\|\mathbf{X} - \mathbf{X}_i\|^3} + \frac{\mathbf{X}_i}{\|\mathbf{X}_i\|^3} \right) \quad (2)$$

For all study cases presented in this paper, the Ephemeris model is limited to the Sun-Earth-Moon system, modelled as point masses using gravitational parameters and states extracted from the DE421 Ephemeris of the *Jet Propulsion Laboratory* (JPL) [6].

NRHOs in the Ephemeris

NRHOs are three-dimensional, periodic orbits of the CR3BP (an example is depicted in Fig. 1.A). This paper will consider exclusively Southern NRHOs about EML-2. Several steps are required to generate long-term NRHO-like orbits in the Ephemeris model:

1. Computing the reference NRHO in the CR3BP.
2. Correcting the CR3BP initial guess in the Ephemeris using time-varying multiple shooting algorithms with stringent epoch continuity constraints [5]. The correction is performed in the J2000 frame, with a precision $\varepsilon_{ms} = 10^{-6}$ for adimensional state discontinuities at the patch points. Orbits obtained are stable for ~ 100 days.
3. Using the result from the multiple shooting correction as a first guess for a receding-horizon procedure. The correction is performed in a rotating reference frame that can locally be compared to the synodic frame. The rotation is such that the primaries will always be aligned with the x-axis of such frame. The receding horizon performs differential correction at the perilune to target a given perilune state N_{LH} revolutions ahead. The orbit is propagated until the next perilune and the process is repeated until stability is guaranteed for the desired amount of revolutions.

This work has used a novel implementation of an adaptive N_{LH} parameter within the receding-horizon procedure. This choice leads to both lower computational strain and station-keeping budgets for orbit maintenance. With this procedure the maintenance budget for a 500-revolutions NRHO orbit with $r_p = 5930 \text{ km}$ (depicted in Fig. 1.B) is equal to 61.729 mm/s , with maximum maneuver amplitude of 0.518 mm/s , which represents a slight improvement with respect to previous implementations found in the literature [2].

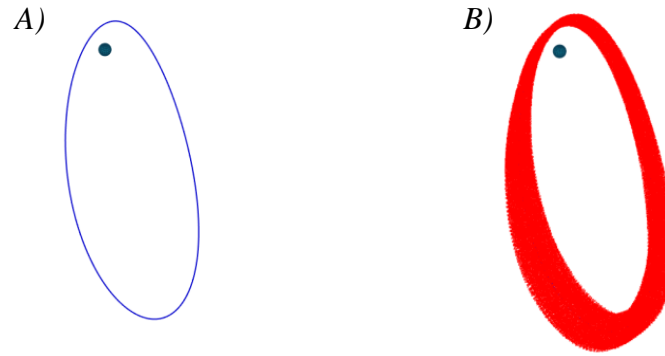


Fig. 1: NRHO in the CR3BP (A) and in the Ephemeris (B)

Natural Drift Far Rendezvous

Natural Drift Approach and Candidate Search

NRHOs are no longer periodic when translated into the Ephemeris model: both chaser and orbit NRHOs present a significant drift with respect to their CR3BP reference in the local rotating frame. The overlapping of chaser and target drifts can be exploited to achieve quasi-free natural far RVD. The aim is for the chaser to reach a region of interest in the vicinity of the target, from where to initiate relative navigation and close-proximity operations. Such region will be referred to as the *approach region*, contained within a distance $75 \text{ km} < d < 100 \text{ km}$ around the target. In the meanwhile, the chaser should avoid entering the *safety region*, defined within a radius of 50 km around the target.

Not all locations along the NRHO are suited for close proximity maneuvers. Near the apolune non-linear terms in the equations of motion, therefore impacts of errors and dispersions, will be much weaker. Consequently only locations with a mean anomaly $\frac{\pi}{2} < \theta < \frac{3\pi}{2}$ will be considered. Different methodologies were used for candidate search, depending on the precision required and the integration time. Local plane search algorithms were used as a first feasibility assessment. More refined, near-neighbour implementations coupled with surface triangulation searches were then applied to obtain the results presented in this paper [7].

In order to differentiate candidates, two criteria are proposed as a first step: the duration of the *opportunity window* when the chaser is within the approach region and its recurrence in case of a no-go (waiting time before another opportunity window is reached).

Safety Analysis

The orbits selected for natural far RVD should also be analysed from a safety point of view. Outside from potential candidate locations, presence of the chaser within the safety region defined previously is unavoidable at certain occurrences, notably near the perilune. One must ensure that such events do not present any major risk of collision. The analysis should also be conducted within the approach region to ensure that the trajectory is passively safe. This work uses estimation techniques commonly used for debris-avoidance analyses [8, 9].

Chaser and target are modelled as spherical objects of radii R_c and R_t . Relative motion is fast enough to be considered linear and positional noises are zero-mean, Gaussian, uncorrelated.

The uncertainty in chaser and target position is modelled as a single combined covariance ellipsoid centered on the chaser, built from the covariance ellipsoids of chaser and target. Collision occurs if the difference in position between chaser and target is less than $R_c + R_t$. Instead of using the full integral expression of the probability of collision P_c , this work relies on an expression of a maximum probability of collision $P_{c,max}$ [8, 9]. For a given aspect ratio

$AR \geq 1$ of the projected covariance ellipsoid in the encounter plane, and a given chaser-target distance d , the maximum probability of collision is given by:

$$P_{c,max} = \left(\frac{\alpha}{1+\alpha}\right) \left(\frac{1}{1+\alpha}\right)^{1/\alpha} \quad (3)$$

Where $\alpha = \frac{(R_c+R_t)^2 AR}{d^2}$. This expression obviously represents an over-estimation of the probability of collision (roughly by two orders of magnitudes). It has both the drawback and benefit of being relatively independent from the covariance (the dependency is present intrinsically in the projected ellipsoid), and it gives us a useful representation of where the “wells” for the full probability of collision might be located with damped computational load.

Simulations and Results

Study Case

A target NRHO with $r_{p,target} = 5930 \text{ km}$ is considered. Such orbit has convenient accessibility constraints, low-instability properties and few eclipses due to its 4:1 resonance with the synodic cycle. The chaser is located on an NRHO with varying perilune radius $4250 \text{ km} < r_{p,chaser} < 5900 \text{ km}$. The reference epoch for orbit generation is set to 2025 NOV 8 23:22:07. Candidates are determined and analysed for 10 target orbit revolutions starting from the reference epoch. For all safety analyses purposes, two different types of error are considered for position dispersion during the encounter: $3\sigma = 1 \text{ km}$ (small error) and $3\sigma = 10 \text{ km}$ (moderate error). The chaser is modelled as a 10 m radius sphere and the target as a 110 m sphere (characteristic dimensions of ATV and ISS respectively).

Natural Far Rendezvous

As $r_{p,chaser}$ tends towards $r_{p,target}$, the number of potential encounters exponentially grows. This exponential trend is more pronounced for near-perilune encounters. To focus on near-apolune encounters, a suitable range appears to be $4750 \text{ km} < r_{p,chaser} < 5300 \text{ km}$. Three regions are of particular interest when looking at the properties of opportunity windows:

1. $4750 \text{ km} < r_{p,chaser} < 5000 \text{ km}$. Within this range, with proper perilune phasing, one can find opportunity windows lasting in average one hour. However, recurrence is low and waiting times are long: 100 hours in average. Only one opportunity can be reasonably exploited without considering re-phasing at the next perilune passage.
2. $5000 \text{ km} < r_{p,chaser} < 5100 \text{ km}$. Range best suited for cargo missions: windows last between 1 and 2 hours with typical recurrence times of 23 to 72 hours.
Example: $r_{p,chaser} = 5080 \text{ km}$ provides 2 opportunity windows lasting 1.08 h and 3.45 h respectively. The waiting time between both windows is 48h.
3. $5100 \text{ km} < r_{p,chaser} < 5300 \text{ km}$. Range best suited for manned missions: windows between 1 and 6 hours, with possibility of recurrence times being less than a day.
Example: $r_{p,chaser} = 5230 \text{ km}$ provides 2 opportunity windows lasting 1.03 and 2.13 h respectively. The waiting time between both windows is about an hour.

Minimum time between RVD windows within the $5000 \text{ km} < r_{p,chaser} < 5230 \text{ km}$ range is presented in Fig. 2. It is important to note, in particular for scenarios involving cargo missions, that a re-phasing maneuver can be performed at the next perilune encounter to accommodate the “drift” of the orbit and prepare for another window. Because the receding-horizon approach presented in this paper considers perilune maintenance maneuvers, different

passages at the perilune tend to be very close to one another and consequently such phasing maneuvers have very low orders of magnitude: a few mm/s for the majority of them.

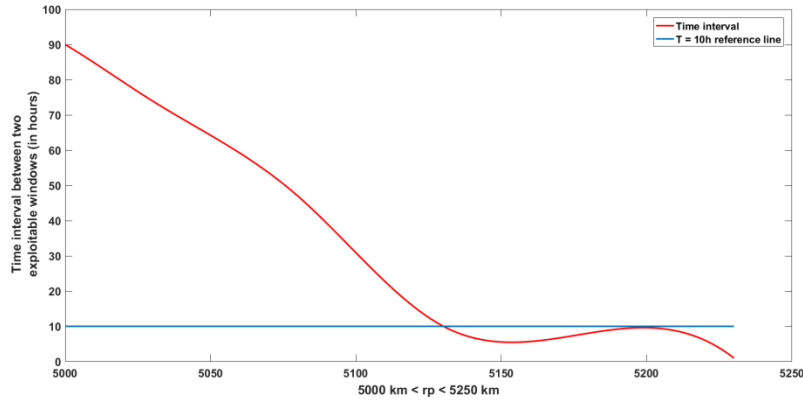


Fig. 2: Minimum time between two natural RVD windows: $5000 \text{ km} < r_{p, \text{chaser}} < 5230 \text{ km}$

Safety Analysis

Small state dispersions cause the target not to intersect with the chaser’s combined covariance ellipsoid in the encounter domain, resulting in a quasi-null probability of collision. Moderate dispersions result in the $P_{c, \text{max}}$ distribution presented in Fig. 3. The value $P_{c, \text{max}} = 6 \cdot 10^{-4}$ is an absolute threshold that seems reasonable (a collisional event occurring roughly every ~450 years), considering the over-estimation of the real probability of collision. Moreover, some regions of interest to minimize $P_{c, \text{max}}$ can be observed around $4750 \text{ km} < r_{p, \text{chaser}} < 4950 \text{ km}$, $r_{p, \text{chaser}} \approx 5000 \text{ km}$, $r_{p, \text{chaser}} \approx 5150 \text{ km}$ and $r_{p, \text{chaser}} \approx 5250 \text{ km}$.

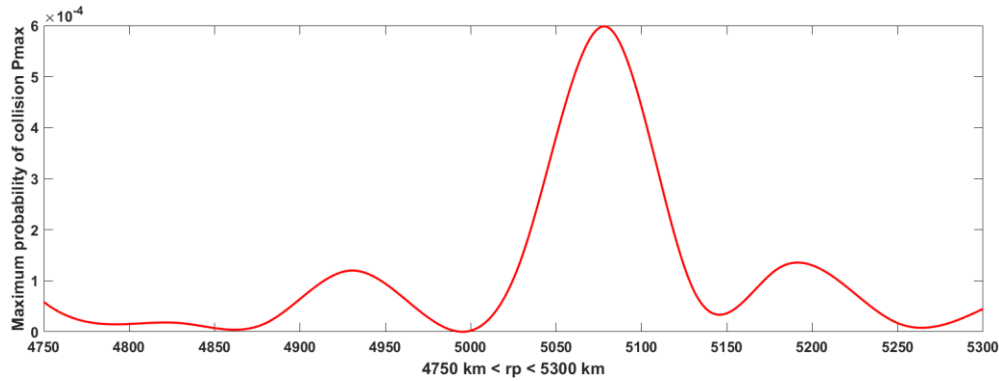


Fig. 3: Maximum probability of collision within the safety region for different $r_{p, \text{chaser}}$

Transition to close-proximity operations

After entering the approach sphere, and in case of a “go” decision, the chaser could engage in relative navigation and start proximity maneuvers (or “close rendezvous”, using the terminology from [3]). This subject has been the scope of previous work by the authors, and is currently investigated. However, one could also complement the natural drift approach with a more traditional trajectory design: a series of impulsive maneuvers within the approach sphere to further approach the target and make the transition to close-rendezvous at a closer relative distance. Two scenarios were considered for this transition: direct transfer at the end of the drift using a Lambert’s arc in the CR3BP corrected in the Ephemeris, and low-energy trajectory design along the invariant manifolds of chaser and target orbits with a Lambert’s arc to connect the manifold branches as a continuation method.

The Lambert’s arc strategy requires a velocity budget between 10 m/s and 100 m/s for transfer durations between two and four hours, depending on the location of the natural drift approach

zone (regions near the apolune require more ΔV). The manifold-to-manifold methodology has more stringent constraints: because the approach region is quite close to the target the optimal solution of such transfer tends towards the pure Lambert's arc solution, with very marginal savings in terms of ΔV and slightly higher time of flights (one to two hours, increases for near-apolune locations). One possible solution to reduce the ΔV budget, at the expense of higher time of flight, is to change the definition of the approach region for the drift and engage the manifold-to-manifold transfer earlier.

Conclusion

This work has presented a novel strategy to design natural drift trajectories in service of far rendezvous operations. The successive steps presented in this paper form a robust methodology to construct quasi-free transfers between NRHO-like orbits in the Ephemeris model, with different possibilities to engage the transition to close-proximity operations. Frequent encounter opportunities are feasible, provided careful selection of the chaser orbit's properties, with waiting times that can be suitable for both manned and cargo flights. A preliminary safety analysis demonstrated that the risk of collision for such operations is very low, and can be further damped. Future research will be oriented towards direct transition to relative navigation within the approach region, at the end of the drift, and the design of a GNC system suited to these kinds of operations.

References

1. S. Lizy-Destrez, "Rendezvous Optimization with an Inhabited Space Station at EML2," in *25th International Symposium on Space Flight Dynamics*, ISSFD, 2015.
2. J. Williams, D.E. Lee, R.J. Whitley, K.A. Bokelmann, D.C. Davis, and C.F. Berry, "Targeting cislunar near rectilinear halo orbits for human space exploration," in *27th AAS/AIAA Space Flight Mechanics Meeting*, 2017.
3. S. Lizy-Destrez, L. Beauregard, E. Blazquez, A. Campolo, S. Manglaviti, and V. Quet, "Rendezvous strategies in the vicinity of the Earth-Moon Lagrangian points," *Frontiers in Astronomy and Space Science*, 2018.
4. W.S. Koon, M.W. Lo, J.E. Marsden, and S.D. Ross, "Dynamical systems, the three-body problem and space mission design," 2017, pp. 26-34.
5. T.A. Pavlak, "Trajectory design and orbit maintenance strategies in multi-body dynamical regimes," 2013.
6. W.M. Folkner, J.G. Williams, and D.H. Boggs, "The planetary and lunar Ephemeris DE 421," Tech. Rep. Vol. 178, Interplanetary Network Progress Report, August 2009.
7. E. Blazquez, L. Beauregard, and S. Lizy-Destrez, "Safe natural far rendezvous approaches for cislunar Near Rectilinear Halo Orbits in the Ephemeris model," in *7th International Conference on Astrodynamics Tools and Techniques*, ICATT, 2018.
8. F.K. Chan, "Spacecraft collision probability," 2008.
9. S. Alfano and D. Oltrogge, "Probability of collision: Valuation, variability, visualization and validity," *Acta Astronautica*, vol. 148, pp. 301–316, 2018.